catalysts

Article

Biochemical Characterisation and Structure Determination of a Novel Cold-Active Proline Iminopeptidase from the Psychrophilic Yeast, *Glaciozyma antarctica* PI12

Shazilah Kamaruddin [1,*], Rohaiza Ahmad Redzuan [1], Nurulermila Minor [1], Wan Mohd Khairulikhsan Wan Seman [2], Mahzan Md Tab [2], Nardiah Rizwana Jaafar [3], Nazahiyah Ahmad Rodzli [2], Mohd Anuar Jonet [2], Izwan Bharudin [1], Nur Athirah Yusof [4], Doris Quay Huai Xia [5], Nor Muhammad Mahadi [2], Abdul Munir Abdul Murad [1] and Farah Diba Abu Bakar [1,*]

1 Department of Biological Sciences & Biotechnology, Faculty of Science and Technology, Universiti Kebangsaan Malaysia, Bangi 43600, Selangor, Malaysia; rohaizaahmadredzuan@gmail.com (R.A.R.); nurulermila@gmail.com (N.M.); ibb@ukm.edu.my (I.B.); munir@ukm.edu.my (A.M.A.M.)
2 Malaysia Genome and Vaccine Institute, Jalan Bangi Lama, Kajang 43000, Selangor, Malaysia; ikhsan@nibm.my (W.M.K.W.S.); mahzan@kimia.gov.my (M.M.T.); nazahiyah@nibm.my (N.A.R.); anuarjonet@nibm.my (M.A.J.); nor.mahadi@gmail.com (N.M.M.)
3 School of Chemical and Energy Engineering, Faculty of Engineering, Universiti Teknologi Malaysia, Skudai 81310, Johor, Malaysia; nardiah@utm.my
4 Biotechnology Research Institute, Universiti Malaysia Sabah, Jalan UMS, Kota Kinabalu 88400, Sabah, Malaysia; nrathirah.yusof@ums.edu.my
5 Department of Applied Physics, Faculty of Science and Technology, Universiti Kebangsaan Malaysia, Bangi 43600, Selangor, Malaysia; dorisquay@ukm.edu.my
* Correspondence: shazilah@ukm.edu.my (S.K.); fabyff@ukm.edu.my (F.D.A.B.)

Citation: Kamaruddin, S.; Ahmad Redzuan, R.; minor, N.; Seman, W.M.K.W.; Md Tab, M.; Jaafar, N.R.; Ahmad Rodzli, N.; Jonet, M.A.; Bharudin, I.; Yusof, N.A.; et al. Biochemical Characterisation and Structure Determination of a Novel Cold-Active Proline Iminopeptidase from the Psychrophilic Yeast, *Glaciozyma antarctica* PI12. *Catalysts* **2022**, *12*, 722. https://doi.org/10.3390/catal12070722

Academic Editors: Cinzia Calvio and Carlo F Morelli

Received: 30 April 2022
Accepted: 28 June 2022
Published: 30 June 2022

Abstract: Microbial proteases constitute one of the most important groups of industrially relevant enzymes. Proline iminopeptidases (PIPs) that specifically release amino-terminal proline from peptides are of major interest for applications in food biotechnology. Proline iminopeptidase has been extensively characterised in bacteria and filamentous fungi. However, no similar reports exist for yeasts. In this study, a protease gene from *Glaciozyma antarctica* designated as *GaPIP* was cloned and overexpressed in *Escherichia coli*. Sequence analyses of the gene revealed a 960 bp open reading frame encoding a 319 amino acid protein (35,406 Da). The purified recombinant *Ga*PIP showed a specific activity of 3561 Umg^{-1} towards L-proline-p-nitroanilide, confirming its identity as a proline iminopeptidase. *Ga*PIP is a cold-active enzyme with an optimum activity of 30 °C at pH 7.0. The enzyme is stable between pH 7.0 and 8.0 and able to retain its activity at 10–30 °C. Although *Ga*PIP is a serine protease, only 25% inhibition by the serine protease inhibitor, phenylmethanesulfonylfluoride (PMSF) was recorded. This enzyme is strongly inhibited by the presence of EDTA, suggesting that it is a metalloenzyme. The dimeric structure of *Ga*PIP was determined at a resolution of 2.4 Å. To date, *Ga*PIP is the first characterised PIP from yeasts and the structure of *Ga*PIP is the first structure for PIP from eukaryotes.

Keywords: microbial proteases; proline specific protease; cold-active enzyme; gluten hydrolysis; protein structure

1. Introduction

Interest in cold-adapted enzymes derived from psychrophilic organisms has increased substantially following reports of their unique attributes and industrial potentials [1]. Thus, these enzymes from psychrophiles have been the focus of many researchers aiming to discover and develop cold-active biocatalysts for scientific studies and industrial applications [2,3]. The ability of psychrophiles to produce novel enzymes and secondary metabolites that facilitate their survival in harsh and cold conditions offers a promising source of industrial enzymes with varying applications in different industrial sectors [4]. As temperature is one of the major external factors affecting the adaptive capability of organisms, enzymes from psychrophiles have evolved functionally and structurally to withstand low-temperature environments [5,6]. These adaptations correspond to key changes in the amino acid sequences, which are translated into variations in the protein structure exhibiting specific flexibility, charge, and/or hydrophobicity of the enzymes [1,7]. Cold-adapted enzymes display useful properties, such as a high catalytic activity at low temperatures and usage of a lower concentration of enzymes for efficient reaction. Thus, heating steps that are expensive and require an enormous amount of thermal energy in industrial settings are eliminated [8]. With the use of cold-adapted enzymes that are environmentally friendly, harsh and noxious chemicals can be replaced to provide a safe environment and healthy living conditions.

Low temperatures disrupt enzyme kinetics whereby a decrease in temperature results in an exponential decrease in reaction rate [7,9]. In contrast, enzymes from psychrophiles show high catalytic efficiency at low-temperature range; temperatures at which their mesophilic and thermophilic counterparts are unable to produce adequate metabolic rates for life support and cell growth [6,10]. Although cold-adapted enzymes can function in the cold, their protein structures are prone to heat-dependent instability, and are thus, heat-labile. Therefore, it is no surprise that many cold-adapted enzymes exhibit low stability at moderate temperatures (usually >40 °C) [11,12].

Proline iminopeptidase (PIP, prolyl aminopeptidase; EC 3.4.11.5) is a unique exopeptidase that catalyses the cleavage of proline from N-terminal peptides [13]. The presence of prolines in polypeptides renders the polypeptides resistant to other proteases [14]. Proline iminopeptidases are known to be involved in the hydrolysis of peptides or proteins, but their biological functions are still unclear. In industries, these enzymes are used as biocatalysts in enhancing the degradation of gluten and collagen in food processing, such as in meat tenderisation and production of gluten-free food, debittering of proteolysates, and flavour development of Swiss-type cheeses ([15–17]). In pharmaceutical and medical applications, PIP can enhance the degradation of gluten, which may cause serious problems for patients suffering from celiac disease. Celiac disease is an intestinal disorder due to an uncontrolled immune response, which is caused by gluten proteins that are resistant to proteolytic degradation within the gastrointestinal tract [18].

Like gluten, collagen is rich in proline and 4-hydroxyproline. Thus, efficient hydrolysis of collagen by PIPs allows it to be used to treat wastewater, particularly in the meat industry, which produces a high amount of collagen [19]. The proteolysis of food proteins like soy protein, gluten, or casein often leads to the release of bitter peptides and negatively influences the products' taste. In this case, PIPs degrade bitter peptides that are usually resistant to hydrolysis by other peptidases [15,16,20].

In light of the proline iminopeptidase industrial benefits, a plethora of molecular characterisation studies have been geared towards the investigation of PIPs from bacteria and fungi, such as *Xanthomonas campestri*, *Aspergillus oryzae*, *Aspergillus niger*, and *Phanerochaete chrysosporium* [19–22]. Despite the presence of comparable PIP genes in the genomes of other green and blue moulds, the gene is absent from the genome of *Saccharomyces cerevisiae*, the most extensively used eukaryotic model organism. Nonetheless, the characterisation of cold-adapted PIPs from psychrophilic yeast has not been described. Therefore, this study aimed to characterise the structural and functional activity of a cold-adapted PIP from a psychrophilic yeast. *Glaciozyma antarctica* PI12 is an obligate psychrophilic yeast isolated from the sea ice of Antarctica with the environment temperature ranging between −20 and 15 °C, and the draft genome was successfully determined and analysed [4]. In this work, we report the biochemical characterisation of a cold-adapted proline iminopeptidase from *G. antarctica* and determine its three-dimensional structure at 2.4 Å resolution. To the best of our knowledge, no cold-adapted proline iminopeptidase structure and function from a psychrophilic yeast has ever been reported. The potential of the recombinant PIP for industrial applications was further evaluated.

2. Results and Discussion

2.1. Cloning and In Silico Analysis of GaPIP G. antarctica

The nucleotide sequence for *GaPIP* was 960 bp, which has been submitted to the GenBank (Accession number MG973064). The gene encoded a 319 amino acid protein with a calculated molecular mass of 35.4 kDa. No signal peptide was predicted for *Ga*PIP; thus, this protein was predicted to be an intracellular protein. Multiple sequence alignment of amino acid sequences revealed that this protein has a similar domain to other PIPs (Figure 1). Amino acid sequence alignment of *Ga*PIP with other known microbial proline aminopeptidases and analysis of conserved domain demonstrated that *Ga*PIP is an α/β-hydrolase fold serine peptidase. It contains a Ser-Asp-His active triad (amino acid positions −111, −269, and −297) and a highly conserved motif G-X-S-X-G to the serine aminopeptidase; GGSWG (Figure 1). In *Aeromonas sobria* and *Bacillus coagulans* PIP, serine residue in the GXSXG motif is responsible for the catalytic activity of the PIP enzymes [23]. In most cases, the GXSXG motif is conserved within multimeric PIPs, but other motifs, such as the GGSWG, GQSWG, and GHSWG, are also found in multimeric PIPs [22]. Based on the phylogenetic analysis, all PIP proteins were grouped according to the number of PIP domains in their structures (Figure 2). The *G. antarctica* PIP was closely related to *Pseudozyma* PIP (Figure 2). This result was expected as both yeasts are classified under the phylum Basidiomycota. Although *Ga*PIP was closely related to the monomeric PIPs with similar conserved motifs, interestingly, *Ga*PIP was found to be in the dimeric form (Section 2.2). This divergence may be due to the sequence evolution or horizontal gene transfer in the yeast genome. In contrast with most bacterial PIPs, a few bacterial PIPs have multimeric domains, such as *A. sobria*, which is similar to the fungi PIPs [22,23].

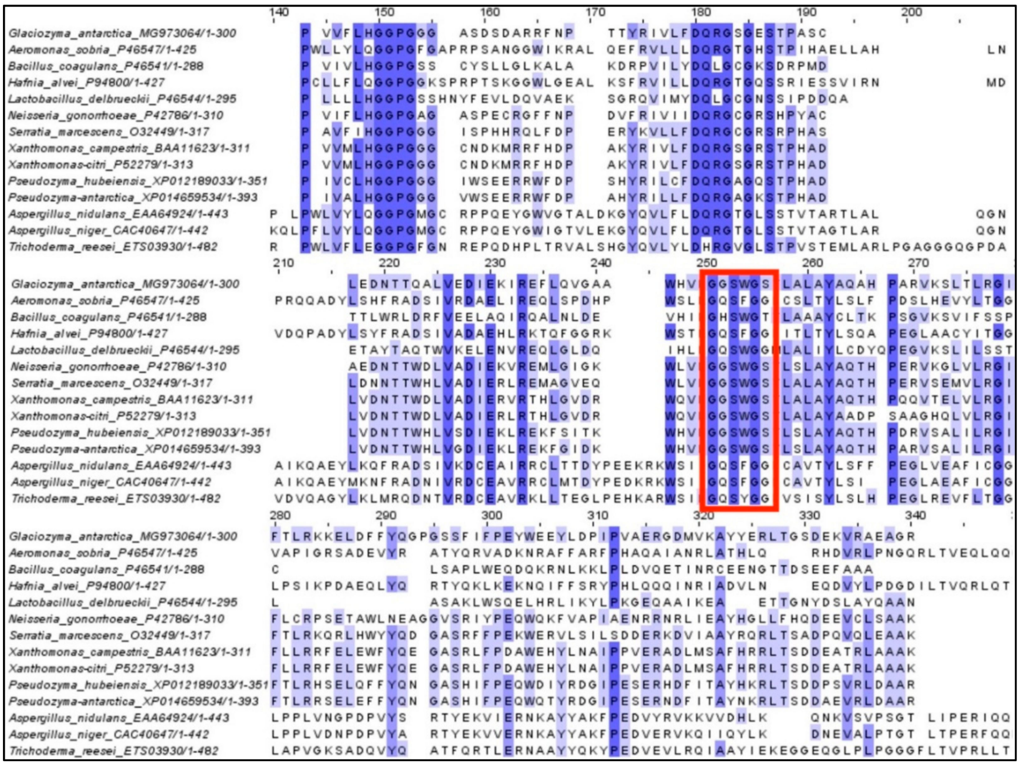

Figure 1. Multiple sequence alignment of catalytic domains of proline iminopeptidases from several monomeric and multimeric sequences obtained from the NCBI. The conserved motif is highlighted with a red box.

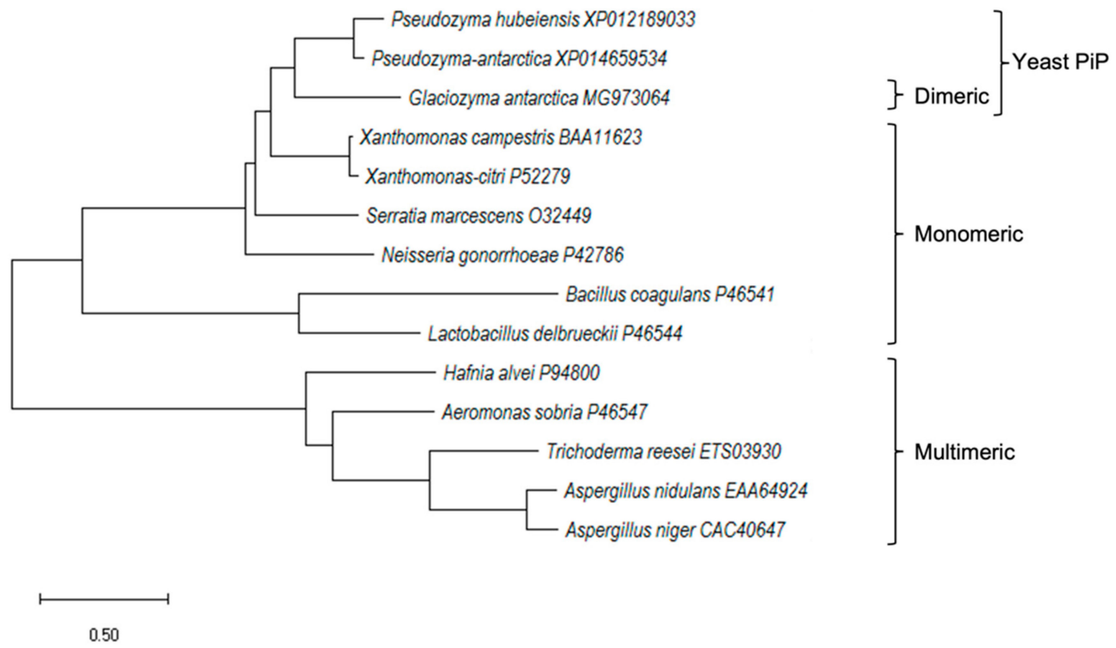

Figure 2. Phylogenetic analyses of proline iminopeptidases from different microorganisms. The phylogenetic tree was constructed using MEGAX software [24].

2.2. Expression of Recombinant GaPIP

The gene encoding for *Ga*PIP was successfully cloned and subsequently used to transform *Escherichia coli* BL21(DE3) cells for expression of the recombinant protein. The optimised expression conditions were at 0.5 mM IPTG and 20 °C for 18 h. The SDS-PAGE analysis of the purified *Ga*PIP showed a single band with an apparent molecular mass of 35 kDa, in agreement with the molecular mass calculated from the open reading frame of the *Ga*PIP nucleotide sequence (Figure 3). The molecular mass of the purified *Ga*PIP, as determined by gel filtration, was ~70 kDa, suggesting that *Ga*PIP is a dimeric enzyme.

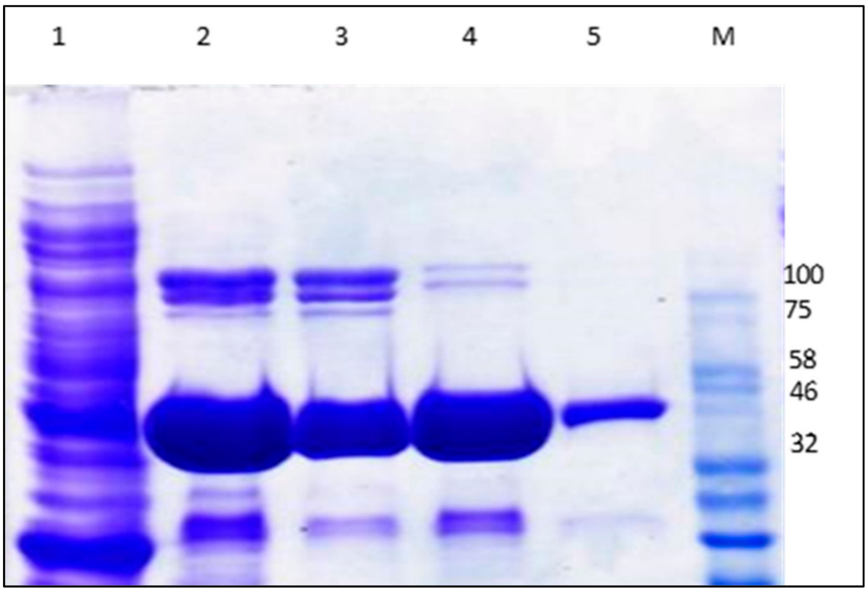

Figure 3. SDS-PAGE profile of the recombinant *Ga*PIP. Lane 1: Whole-cell protein extract of *Ga*PIP expressed in *E. coli* BL21(DE3) STAR; Lane 2: Purified *Ga*PIP using Ni-NTA; Lane 3–5: Purified *Ga*PIP using gel filtration chromatography from different elution; M: Protein Marker Broad Range (NEB, Ipswich, MA, USA).

2.3. Biochemical Properties of GaPIP

The purified *Ga*PIP had a maximum activity at 30 °C. The enzyme was active at a temperature range from 10 to 60 °C. An increase in temperature resulted in a decrease in *Ga*PIP activity (Figure 4a). *Ga*PIP showed high stability in response to heat treatment for 30 min at temperatures below 30 °C but drastically lost activity at temperatures over 30 °C (Figure 4b), suggesting that this cold-active enzyme exhibited low structural stability to compensate for its maximal activity at temperatures below 30 °C [25]. *Ga*PIP may have exhibited weak intramolecular interactions and less core hydrophobicity in its protein structural characteristics, which led to a lack of structural rigidity. It has been proposed that increased flexibility is the most important factor for the catalytic efficiency of psychrophilic enzymes at low temperatures, which enhances the efficiency of substrate binding to the enzyme catalytic site [6]. Cold-adapted enzymes show high flexibility and compensate for the low kinetic energy present in cold environments, thus reducing activation energy compared to their mesophilic and thermophilic homologues [26]. As for the effect of pH, *Ga*PIP showed optimum activity at pH 7 (Figure 5a). In addition, about 50% to 97% of its optimum activity was still detectable at pH ranging between 4 and 7. The pH stability of *Ga*PIP was assessed and it demonstrated enzyme stability at pH 7–8 by retaining more than 60% residual activity (Figure 5b).

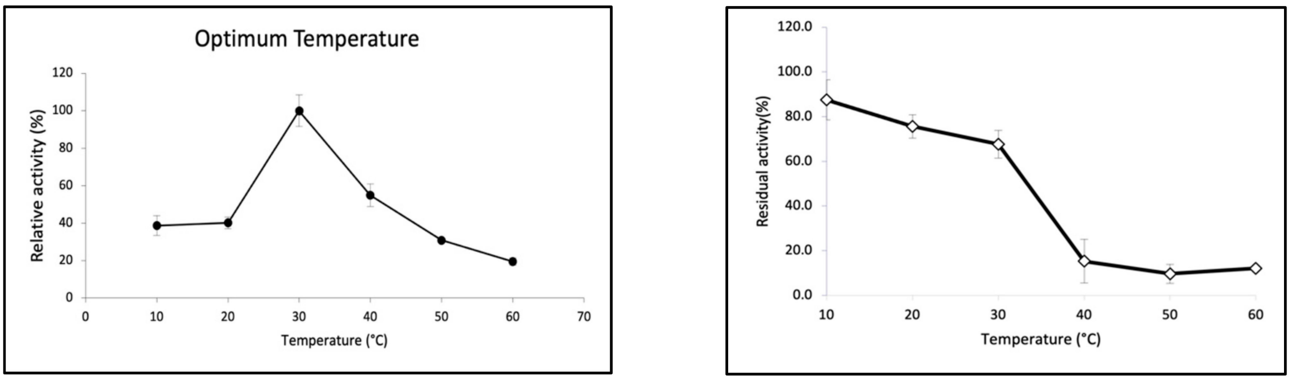

(**a**) (**b**)

Figure 4. Effect of temperature on enzyme (**a**) activity and (**b**) stability of purified *Ga*PIP. The optimal temperature was determined by measuring the enzymatic activity and stability at different temperatures ranging from 0 to 60 °C. The error bars represent the standard deviation (n = 3).

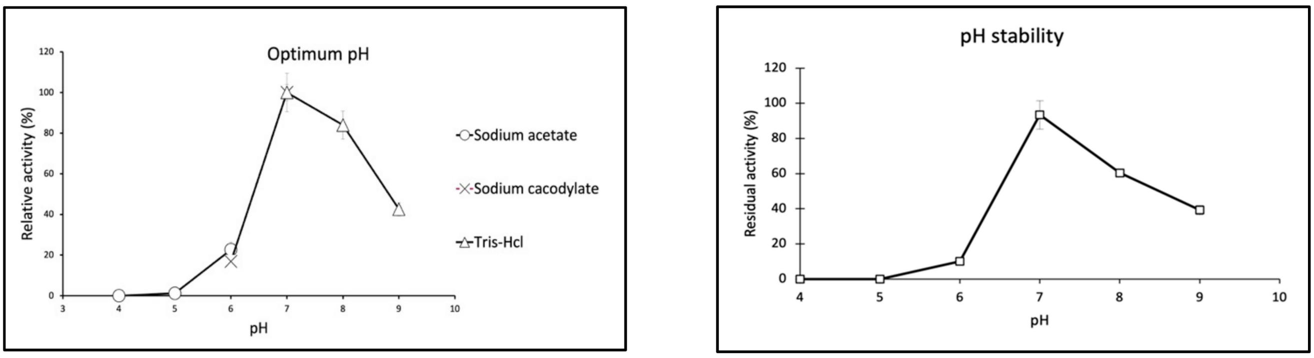

(**a**) (**b**)

Figure 5. Effect of pH on enzyme (**a**) activity and (**b**) stability of purified *Ga*PIP. The optimal pH was determined by measuring enzyme activity in different buffer systems ranging from pH 3 to 9. The pH stability was determined by incubating an enzyme at different buffers for 30 min. The error bars represent the standard deviation (n = 3).

The hydrolytic activity of *Ga*PIP was determined in the presence of different protease inhibitors, metal ions, and chemical reagents. As shown in Figure 6, *Ga*PIP was completely inactivated by several divalent cations, such as Mn^{2+}, Zn^{2+}, Co^{2+}, and Ni^{2+}, whilst Mg^{2+} significantly improved the activity of *Ga*PIP. Metal chelator (EDTA) partially affected the enzyme activity, which indicated that the *Ga*PIP was a metal-dependent enzyme and required metal ions for enhanced performance. No inhibition of enzyme activity was observed in the presence of reducing reagents, dithiothreitol (DTT), but interestingly, β-mercaptoethanol significantly enhanced the activity. This result suggested that *Ga*PIP is likely to be an aminopeptidase and the presence of disulphide bonds in the structure did not exhibit any crucial role in the catalytic activity of *Ga*PIP. This enzyme was slightly inhibited by a potent serine protease inhibitor, phenylmethanesulfonylfluoride (PMSF) with only 25% inhibition and to a lesser extent by iodoacetamide.

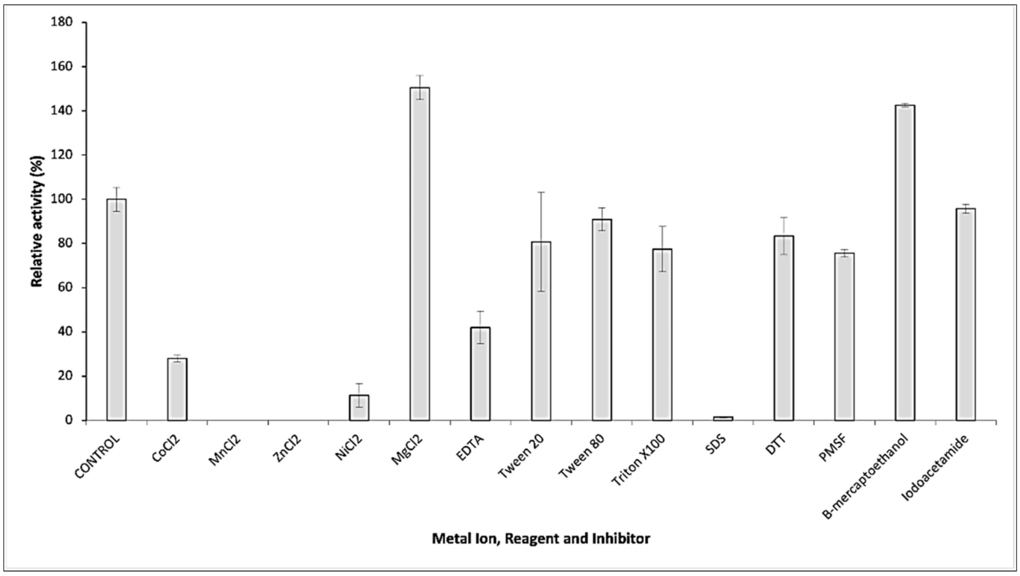

Figure 6. Effect of metal ions, reagents, and inhibitors on the activity of purified *Ga*PIP. The relative activity of the unincubated enzyme without metal ions, reagents, and inhibitors (control) was taken at 100%. The error bars represent the standard deviation (n = 3).

Several substrates were tested to determine the substrate specificity of *Ga*PIP (Table 1). The data obtained indicated that *Ga*PIP was strictly an exopeptidase as it failed to cleave N-substituted prolyl peptides (N-succinyl-Ala-Ala-Pro-Leu-p-nitroanilide) and could only release proline monomers from poly-L-proline (L-Pro-pNA). Moreover, the enzyme was active in cleaving Met-pNA and Ala-pNA, but no detectable activity was observed towards Leu-pNA. This broad substrate specificity was somewhat different from other eukaryotic fungal PIPs (i.e., *A. niger* and *A. oryzae*) that can only hydrolyse L-Pro-pNA and hydroxy-Pro-pNA [20,22,27]. However, the specificity of *Ga*PIP was similar to other bacterial PIPs, such as *X. campestris* and *S. marcescens* which can release alanine residues from the aminopeptides [21,28]. In contrast to other fungal and bacterial PIPs, *Ga*PIP hydrolysed Ala-pNA more efficiently than L-Pro-pNA with higher catalytic efficiency and specific activity.

Table 1. Kinetic parameters of *Ga*PIP.

Substrate	K_m (mM)	V_{max} (nmole min^{-1})	K_{cat} (s^{-1})	K_{cat}/K_m (mM^{-1} s^{-1})	Specific Activity (Umg^{-1})
L-Proline-p-nitroanilide-trifluoroacetate	1.012	3.561	2.08	2.05	3561
L-Methionine-p-nitroanilide	1.321	1.783	1.04	0.79	1783
L-Alanine-p-nitroanilide	4.088	4.891	14.3	3.49	48,900
L-Leucine-p-nitroanilide	N.D.	N.D.	N.D.	N.D.	N.D.
N-succinyl-Ala-Ala-Pro-Leu-p-nitroanilide	N.D.	N.D.	N.D.	N.D.	N.D.

N.D.: Not determined due to no activity.

2.4. Structure Determination of GaPIP

G. antarctica PI12 proline iminopeptidase was successfully crystallised in 30% PEG 4000, 0.2 M ammonium acetate, and 0.1 M sodium citrate using vapour diffusion. The crystal was diffracted to 2.4 Å resolution and belonged to space group P21221. Crystallographic analysis revealed that the solvent content was 50.03% and its Matthew's coefficient was 2.46 Å^3 Da^{-1}. Analyses of the crystal structure revealed a citrate anion in the active site of *Ga*PIP of both chains. The ligand interacted with His297, a residue of the catalytic triad. The orientation and conformation of the residues interacting with the citrate anion may resemble ligand binding.

Structure determination of *Ga*PIP was performed by molecular replacement using *X. campestris* PIP structure (PDB ID: 1AZW; [29]) and this structure has been deposited in PDB (PDB ID: 5YHP) (Figure 7). It was also shown that *Ga*PIP has nine clefts and two pores. The catalytic triads (Ser111, Asp269, and His297) were located on the surface of the largest cleft, thus providing access for a substrate to enter the active site of *Ga*PIP.

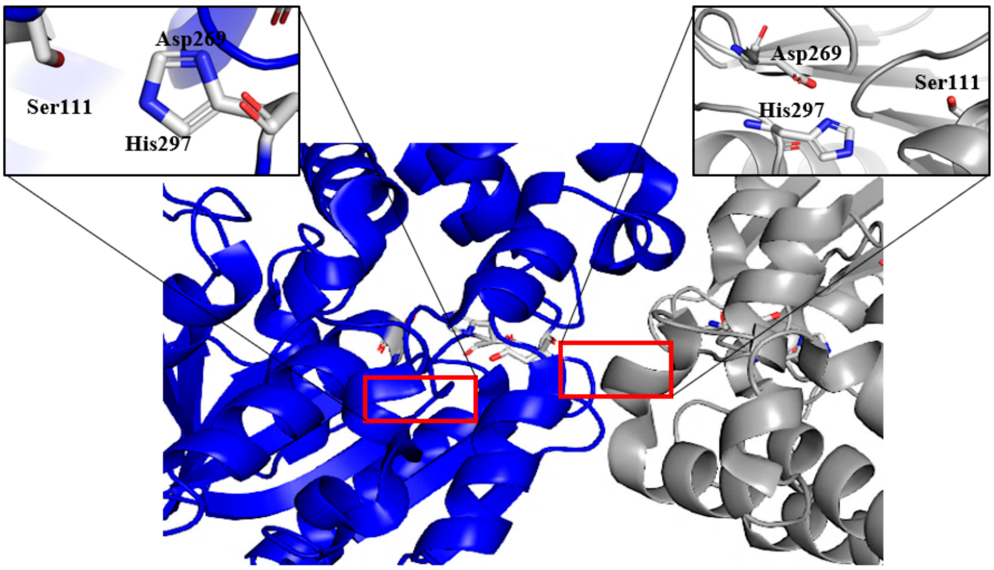

Figure 7. The overall structure of *Ga*PIP at 2.4 Å. Chain A (grey) and Chain B (blue) are represented by different colours. The catalytic triads of the dimeric *Ga*PIP structures are shown in boxes.

Structural analysis revealed that the psychrophilic *Ga*PIP (5YHP) has similar features to 1AZW, which was isolated from a mesophilic bacterium (Table 2).

Table 2. Structural and interaction comparison between *Ga*PIP (5YHP) and 1AZW.

	***Ga*PIP**	**1AZW**
Total number of amino acids		
Glycine (%)	8.2	7.7
Proline (%)	6.3	5.1
Arginine (%)	5.6	7.3
Hydrophobic interactions	526	528
Hydrogen bonds (MC-MC)	807	769
Hydrogen bonds (MC-SC)	271	285
Hydrogen bonds (SC-SC)	202	290
Ionic interactions	89	86
Aromatic-aromatic interactions	50	40
Aromatic-sulphur interactions	4	5
Cation-pi interactions	10	6
Intraprotein disulphide bridges	0	0
Pocket (cavity) numbers	5	4
Exposed surface area (Å^2)		
Total	23,374.4	23,500.9
Polar	3636.0	3747.7
Non-polar	14,489.7	13,361.8

No additional loops (one of the structural traits of psychrophilic enzymes) were displayed on *Ga*PIP that may contribute to an increase in its structural architecture flexibility. However, *Ga*PIP possesses additional cavities (five cavities) and has a larger non-polar solvent accessible surface area (14,489.7 Å^2) as compared to 1AZW. An increased number of cavities and larger non-polar exposed surface area was found to enhance the conformational dynamics that lead to more water molecules in the structure, thus increasing the global flexibility of the enzyme [30,31]. In addition, it was also shown that *Ga*PIP has a higher percentage of glycine (8.2%) and a lower percentage of arginine (5.6%) in comparison to 1AWZ (7.7% glycine and 7.3% arginine). An increased number of glycines and reduction in arginine content provide local mobility and enhance flexibility between secondary structures in psychrophilic proteins [25,32].

The structure of *Ga*PIP encompassed all 319 amino acid residues of the enzyme and the presence of two monomeric domains of *Ga*PIP indicated that it existed as a dimer in solution. The dimeric interaction of the two domains retained at least 150 direct atom contacts that included polar and nonpolar interactions (Figure 8a). *Ga*PIP shared similar topological features with 1AZW (Figure 8b) with an RMSD of 0.6 Å, and the sequence similarity between the two was approximately 56%.

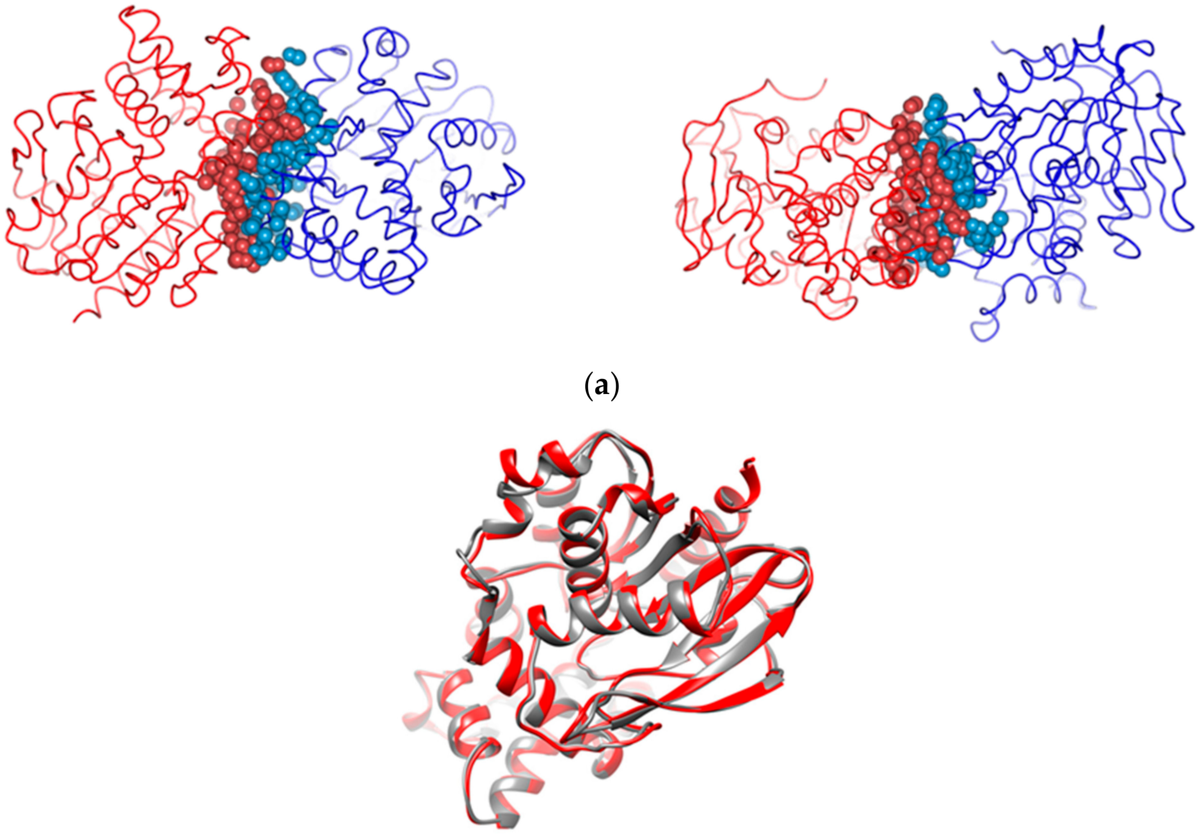

(**a**)

(**b**)

Figure 8. (**a**) The dimeric assemblies of *Ga*PIP at different orientations. Atoms involved in dimer formations are highlighted in spheres. Each colour represents one monomer. (**b**) Superimposed structures of the solved *Ga*PIP–5YHP (red ribbon) and the 1AZW structure (grey ribbon) at an RMSD of 0.6 Å.

3. Materials and Methods

3.1. Microorganism and Culture Conditions

The psychrophilic yeast, *G. antarctica* PI12 was obtained from the Antarctic Microbial Culture Collection of the School of Biological Sciences, Universiti Sains Malaysia, Penang, Malaysia. It was grown in a YPD medium containing 25 µg/mL ampicillin and 25 µg/mL kanamycin (2% peptone, 1% yeast extract, 1% dextrose) for 7 days at 12 °C. For RNA extraction, fungal mycelia were harvested after 48 h of growth by filtration with filter paper, frozen with liquid nitrogen, and stored at −80 °C until further use.

3.2. Total RNA Isolation and cDNA Synthesis

A total of 2 g of the frozen cells was ground to a fine powder using RNAse-free mortar and pestle. Total RNA was extracted according to the method described by Bharudin et al., 2014 [33]. cDNAs were synthesised using Superscript III First-Strand cDNA Synthesis Kit (Invitrogen Life Technologies, Grand Island, NY, USA). The primers were designed based on the genome database of *G. antarctica* available at GenBank via the accession number ASRT0000000 [4]. The sequence of the forward primer was 5′ATGACCTCCCTCTTCGCCGC CATCC 3′ and the reverse primer was 5′CTACGCGAGCTTCGCAAACTCCTCC 3′. PCR was performed using a Taq DNA Polymerase Kit (Invitrogen Life Technologies, Grand Island, NY, USA). PCR was commenced with a pre-denaturation step at 94 °C for 4 min, followed by 30 cycles of denaturation (94 °C, 1 min), annealing (50 °C, 1 min), and extension (72 °C, 2 min). The final extension was conducted at 72 °C for 7 min. The amplified cDNA was cloned into a pGEMT-Easy vector (Promega, Madison, WI, USA) and sequenced using SP6 and T7 universal primers (Promega, Madison, WI, USA).

3.3. Alignment of Protein Sequences and Phylogenetic Reconstruction

The Muscle programme [34] was used for multiple alignments of protein sequences using the default parameters and the alignment was presented using the Jalview programme [35]. MEGAX package was used for the phylogenetic reconstruction analysis [24]. To assess the internal support of tree branches, heuristic bootstrap analyses with 1000 replicates were performed. Table 3 shows the list of PIP proteins used in the phylogenetic analysis. The sequence obtained was also analysed with several online bioinformatics tools, such as SignalP-6.0 (https://services.healthtech.dtu.dk/service.php/SignalP (accessed on 12 April 2019)), Wolf Psort (https://wolfpsort.hgc.jp/ (accessed on 12 April 2019)) and Phobius (https://phobius.sbc.su.se/ (accessed on12 April 2019)) to predict the presence of signal peptide.

Table 3. List of proline iminopeptidase proteins used in the phylogenetic analysis.

Group	Nomenclature Species	Accession No
Bacteria	*Aeromonas sobria*	P46547
	Bacillus coagulans	P46541
	Hafnia alvei	P94800
	Lactobacillus delbrueckii	P46544
	Neisseria gonorrhoeae	P42786
	Serratia marcescens	O32449
	Xanthomonas campestris	BAA11623
	Xanthomonas citri	P52279
Yeasts	*Pseudozyma hubeiensis*	XP 012189033
	Pseudozyma antarctica	XP 014659534
Fungi	*Aspergillus nidulans*	EAA64924
	Aspergillus niger	CAC40647
	Trichoderma reesei	ETS03930

3.4. Construction of Expression Vectors

Construction of expression vectors was performed using plasmids carrying *Ga*PIP cDNA as a template. PCR was performed using this template to amplify a fragment encoding the mature *Ga*PIP with the forward primer, including the sequence of CACC before the start codon to allow directional cloning into the prokaryotic expression vector, pET200/D-TOPO® (Invitrogen Life Technologies, Grand Island, NY, USA). The PCR mixture contained 2 µL of first-strand cDNA, 1 × PCR Buffer, 2 mM dNTP, 20 pmol forward and reverse primers, 25 mM $MgSO_4$, and 1.0 µL KOD Hotstart DNA polymerase (Invitrogen Life Technologies, Grand Island, NY, USA). PCR was performed as follows: initial denaturation at 95 °C for 2 min, followed by 30 cycles of denaturation at 95 °C for 20 s, annealing at 50 °C for 10 s, and elongation at 72 °C for 15 s. The fragment was cloned into pET200/D-TOPO fused with a His_6 tag at the N terminus of the inserted gene product. BL21(DE3) Star One-Shot *E. coli* cells (provided in the pET200/D-TPOPO kit) were transformed with the pET200/*Ga*PIP plasmid. The positive clones were selected using PCR analysis and the recombinant plasmids were extracted and confirmed by double digestion. In addition, the native pET200/D/lacZ vector, without the inserted DNA, was used to transform the same host and was subsequently used as a control for protein expression.

3.5. Expression of the GaPIP in E. coli BL21(DE3) Star

E. coli BL21(DE3) Star harbouring *Ga*PIP in the pET200 vector was inoculated into 5 mL Luria-Bertani (LB) liquid media containing kanamycin (25 µg mL^{-1}) on a rotary shaker (220 rpm) for 18 h at 37 °C, which was used as seed. The prepared seed was inoculated into 50 mL (250 mL shaker flask) LB liquid media containing kanamycin (25 µg mL^{-1}) on a rotary shaker (220 rpm) at 37 °C until the optical density at 600 nm reached 0.6–0.8. IPTG was added with a final concentration of 0.5 mM and the culture temperature was changed from 37 to 20 °C. The cultivation was continued for 18 h and cells were harvested by centrifugation. Harvested cells were resuspended in lysis buffer (50 mM Tris-HCl pH 7.0) and disrupted by three cycles of sonication (10 s per cycle). Cell debris was then treated with 250 U μL^{-1} of benzonase (Merck-Millipore, Darmstadt, Germany) before centrifuging at 10,000× *g* for 20 min at 4 °C. SDS-PAGE was performed using 12.5% polyacrylamide gels and subsequently stained with Coomassie brilliant blue R250.

3.6. Purification of Recombinant GaPIP

Crude extracts of recombinant *Ga*PIP were purified using affinity chromatography and gel filtration. Recombinant *Ga*PIP protein fused with a 6× histidine tag was subjected to Ni-NTA Sepharose column purification using an AKTA Prime System (Amersham, Buckinghamshire, UK). In this method, the recombinant proteins were eluted based on the difference in the affinity to nickel ions between the histidine-tagged recombinant protein and other *E. coli* proteins. *Ga*PIP recombinant protein was eluted using 20 mM imidazole (Acros Organics, Geel, Antwerp, Belgium) in binding buffer pH 7.4 and 500 mM imidazole in elution buffer pH 7.4. The fractions were further chromatographed on a Superdex 200 10/300 GL (GE Healthcare, Buckinghamshire, UK) column using 50 mM Tris-HCl buffer (pH 7.0) as the elution buffer. The detection of PIP activity was carried out using L-proline-p-nitroanilide-trifluoroacetate as a substrate for the enzymatic reaction. Active fractions were pooled and concentrated by ultrafiltration. The target protein fractions were pooled and analysed by 12% SDS-PAGE and Western blot.

3.7. Biochemical Characterisation of GaPIP

The amount of recombinant *Ga*PIP produced was measured using the The Quick Start™ Bradford Protein Assay (Bio-Rad, Hercules, CA, USA). The intact mass of *Ga*PIP was determined using the Agilent 1290 Infinity LC system coupled to Agilent 6520 Accurate-Mass Q-TOF mass spectrometer with a dual ESI source (Agilent Technologies, Santa Clara, CA, USA). Enzymes were assayed using L-proline-p-nitroanilide-trifluoroacetate (Sigma Aldrich, St. Louis, MO, USA) as a substrate. The PIP assay was carried out by adding approximately 1 µg of purified *Ga*PIP to 490 µL of 5 mM L-proline-p-nitroanilide-trifluoroacetate in 50 mM Tris-HCl buffer pH 7.0. The reaction mixture was incubated at 30 °C for 10 min and terminated by the addition of 500 µL of 1 M sodium carbonate. The release of p-nitrophenol was monitored at 405 nm. One unit of PIP activity was defined as the amount of enzyme that produced 1.0 nmol of p-nitrophenol per minute under standard assay conditions. The effects of temperature and pH on *Ga*PIP activities were characterised at temperatures of 10–70 °C and pH 3–8, respectively. Temperature and pH stability were assessed, respectively, by incubating the enzyme at pH 7 for 30 min at different temperatures (10–70 °C) and by incubating at 30 °C for 30 min at different pH values (pH 3.0–9.0). The residual activity of the pre-incubated enzyme was then determined using standard assay conditions. The effects of protease inhibitors (PMSF, DTT, and iodoacetamide), reagents (EDTA, Urea, SDS, Triton X100, Tween 20, and Tween 80), and metal ions (Mg^{2+}, Co^{2+}, Zn^{2+}, Fe^{2+}, Mn^{2+}, and Ni^{2+}) on the activity of the purified enzyme were analysed using L-proline-p-nitroanilide-trifluoroacetate as a substrate. The reaction mixture consisted of 1 µg of purified *Ga*PIP in 50 mM Tris-HCl buffer pH 7.0 containing 5 mM final concentration of 5 mM of metal ions/inhibitors or 1% reagents. The enzyme activity in the absence of both metal ions and protease inhibitors served as the control.

3.8. Substrate Specificity and Kinetic Parameters

The Michaelis-Menten constant (K_m) and maximum velocity of substrate hydrolysis (V_{max}) were determined from a Lineweaver-Burk plot. The reactions were performed by incubating 10 µL of purified *Ga*PIP with 490 µL of 50 mM Tris-HCl buffer pH 7.0 with various ranges of substrate concentrations at 30 °C for 30 min. The substrates used were L-proline-p-nitroanilide-trifluoroacetate, L-methionine-p-nitroanilide, L-alanine-p-nitroanilide, L-leucine-p-nitroanilide, N-succinyl-Ala-Ala-Pro-Leu-p-nitroanilide, and N-succinyl-gly-gly-Phe-Leu-p-nitroanilide (Sigma Aldrich, St. Louis, MO, USA). The catalytic constant (K_{cat}) and the specificity constant (K_{cat}/K_m) were calculated. All experiments were carried out with three technical replicates and two biological replicates. The substrate affinity (K_m) and velocity of catalysis (V_{max}) values were calculated by fitting appropriate Michaelis-Menten equations to the data by using nonlinear regression in GraphPad Prism 5 software (San Diego, CA, USA).

3.9. Crystallisation, Data Collection, and Structure Determination

Crystallisation experiments were set up using the hanging drop vapour-diffusion method according to Jaafar et al., 2016 [36]. Crystals suitable for diffraction were grown in 30% PEG 4000, 0.2 M ammonium acetate, and 0.1 M sodium citrate. After one month of incubation, it was transferred into a cryoprotectant solution consisting of the mother liquor and 23% (v/v) glycerol and flash-cooled in liquid nitrogen in a mounted cryo-loop. Diffraction data of *Ga*PIP were collected at MGVI's in-house X-ray facility. The data were indexed, integrated, and scaled using the programme HKL-3000 (Minor et al., 2006). The structure of *Ga*PIP was determined by molecular replacement using the coordinates of *X. campestris* proline iminopeptidase (PDB ID: 1AZW). The structure model was built and refined with the PHENIX suite [37]. The final data-collection and processing statistics are summarised in Supplementary Information Table S1.

4. Conclusions

In conclusion, *Ga*PIP was biochemically and structurally characterised as a cold-active PIP, with a dimeric conformation, Mg^{2+}-dependent, and optimally active at 30 °C and pH 7.0. This enzyme has a broad specificity for substrates, including L-alanine-p-nitroanilide, L-proline-p-aniline, and L-methionine-p-nitroanilide. This broad substrate specificity may be involved in mediating the survivability of *G. antarctica* in the cold environment by metabolising different peptides as carbon sources. The relationship between protein structural flexibility and several other structural factors of *Ga*PIP with its cold-active catalytic activity is yet to be explored further. Insights into this association will enhance the understanding of the structure-function relationships of low-temperature-active enzymes and facilitate applications in selected industries. This is the first report of a cold-adapted PIP from *Glaciozyma* species isolated from the Antarctic sea.

Supplementary Materials: The following supporting information can be downloaded at: https://www.mdpi.com/article/10.3390/catal12070722/s1, Table S1: Data collection, processing and structure refinement.

Author Contributions: Conceptualization, S.K. and F.D.A.B.; Formal analysis, R.A.R.; Funding acquisition, N.M.M., A.M.A.M. and F.D.A.B.; Methodology, S.K., N.A.R., N.M., W.M.K.W.S., N.R.J., M.A.J., M.M.T. and I.B.; Project administration, N.M.M., A.M.A.M. and F.D.A.B.; Supervision, N.M.M., A.M.A.M. and F.D.A.B.; Writing—original draft, S.K.; Writing—review and editing, S.K., N.A.R., N.R.J., R.A.R., I.B., D.Q.H.X., N.A.Y., A.M.A.M. and F.D.A.B. All authors have read and agreed to the published version of the manuscript.

Funding: This research was funded by Universiti Kebangsaan Malaysia, grant number GUP-2020-044 & GGPM-2017-063 and The ministry of Science, Technology and Innovation Malaysia, grant number 02-05-20-SF0007.

Data Availability Statement: The data presented in this study are available in supplementary material.

Acknowledgments: The authors would like to thank the Synchrotron Light Research Institute (BL7.2W) (Public Organization), Nakhon Ratchasima, Thailand, for providing access to and support in the synchrotron facility.

Conflicts of Interest: The authors declare no conflict of interest.

References

1. Sarmiento, F.; Peralta, R.; Blamey, J.M. Cold and Hot Extremozymes: Industrial Relevance and Current Trends. *Front. Bioeng. Biotechnol.* **2015**, *3*, 148. [CrossRef] [PubMed]
2. Moon, S.; Kim, J.; Bae, E. Structural Analyses of Adenylate Kinases from Antarctic and Tropical Fishes for Understanding Cold Adaptation of Enzymes. *Sci. Rep.* **2017**, *7*, 16027. [CrossRef] [PubMed]
3. Raddadi, N.; Cherif, A.; Daffonchio, D.; Neifar, M.; Fava, F. Biotechnological Applications of Extremophiles, Extremozymes and Extremolytes. *Appl. Microbiol. Biotechnol.* **2015**, *19*, 7907–7913. [CrossRef] [PubMed]
4. Firdaus-Raih, M.; Hashim, N.H.F.; Bharudin, I.; Abu Bakar, M.F.; Huang, K.K.; Alias, H.; Lee, B.K.B.; Mat Isa, M.N.; Mat-Sharani, S.; Sulaiman, S. The *Glaciozyma antarctica* Genome Reveals an Array of Systems That Provide Sustained Responses towards Temperature Variations in a Persistently Cold Habitat. *PLoS ONE* **2018**, *13*, e0189947. [CrossRef] [PubMed]
5. Struvay, C.; Feller, G. Optimization to Low Temperature Activity in Psychrophilic Enzymes. *Int. J. Mol. Sci.* **2012**, *13*, 11643–11665. [CrossRef] [PubMed]
6. Yusof, N.A.; Hashim, N.H.F.; Bharudin, I. Cold Adaptation Strategies and the Potential of Psychrophilic Enzymes from the Antarctic Yeast, *Glaciozyma antarctica* Pi12. *J. Fungi* **2021**, *7*, 528. [CrossRef]
7. Åqvist, J.; Isaksen, G.V.; Brandsdal, B.O. Computation of Enzyme Cold Adaptation. *Nat. Rev. Chem.* **2017**, *1*, 51. [CrossRef]
8. Siddiqui, K.S. Some like It Hot, Some like It Cold: Temperature Dependent Biotechnological Applications and Improvements in Extremophilic Enzymes. *Biotechnol. Adv.* **2015**, *33*, 1912–1922. [CrossRef]
9. Marx, J.C.; Blaise, V.; Collins, T.; D'Amico, S.; Delille, D.; Gratia, E.; Hoyoux, A.; Huston, A.L.; Sonan, G.; Feller, G. A Perspective on Cold Enzymes: Current Knowledge and Frequently Asked Questions. *Cell. Mol. Biol. (Noisy-Grand)* **2004**, *50*, 643–655.
10. Santiago, M.; Ramírez-Sarmiento, C.A.; Zamora, R.A.; Parra, L.P. Discovery, Molecular Mechanisms, and Industrial Applications of Cold-Active Enzymes. *Front. Microbiol.* **2016**, *7*, 1408. [CrossRef]
11. Tattersall, G.J.; Sinclair, B.J.; Withers, P.C.; Fields, P.A.; Seebacher, F.; Cooper, C.E.; Maloney, S.K. Coping with Thermal Challenges: Physiological Adaptations to Environmental Temperatures. *Compr. Physiol.* **2012**, *2*, 2151–2202. [PubMed]
12. Nandanwar, S.K.; Borkar, S.B.; Lee, J.H.; Kim, H.J. Taking Advantage of Promiscuity of Cold-Active Enzymes. *Appl. Sci.* **2020**, *10*, 8128. [CrossRef]
13. Rawlings, N.D.; Salvesen, G. *Handbook of Proteolytic Enzymes*; Elsevier: Amsterdam, The Netherlands, 2013; Volume 3, pp. 2491–2523.
14. Omar, M.N.; Rahman, R.N.Z.R.A.; Noor, N.D.M.; Latip, W.; Knight, V.F.; Ali, M.S.M. Structure-Function and Industrial Relevance of Bacterial Aminopeptidase p. *Catalysts* **2021**, *11*, 1157. [CrossRef]
15. FitzGerald, R.J.; O'Cuinn, G. Enzymatic Debittering of Food Protein Hydrolysates. *Biotechnol. Adv.* **2006**, *24*, 234–237. [CrossRef]
16. Cheung, L.K.Y.; Aluko, R.E.; Cliff, M.A.; Li-Chan, E.C.Y. Effects of Exopeptidase Treatment on Antihypertensive Activity and Taste Attributes of Enzymatic Whey Protein Hydrolysates. *J. Funct. Foods* **2015**, *13*, 262–275. [CrossRef]
17. Chanalia, P.; Gandhi, D.; Attri, P.; Dhanda, S. Extraction, Purification and Characterization of Low Molecular Weight Proline Iminopeptidase from Probiotic *L. plantarum* for Meat Tenderization. *Int. J. Biol. Macromol.* **2018**, *109*, 651–663. [CrossRef]
18. Dunaevsky, Y.E.; Tereshchenkova, V.F.; Belozersky, M.A.; Filippova, I.Y.; Oppert, B.; Elpidina, E.N. Review Effective Degradation of Gluten and Its Fragments by Gluten-Specific Peptidases: A Review on Application for the Treatment of Patients with Gluten Sensitivity. *Pharmaceutics* **2021**, *13*, 1603. [CrossRef]
19. Liu, D.; Zhang, D.; Huang, Q.; Gu, L.; Zhou, N.; Tian, Y. Mutagenesis for Improvement of Activity and Stability of Prolyl Aminopeptidase from *Aspergillus oryzae*. *Appl. Biochem. Biotechnol.* **2020**, *191*, 1483–1498. [CrossRef]
20. Li, N.; Wu, J.; Zhang, L.; Zhang, Y.; Feng, H. Biochimie Characterization of a Unique Proline Iminopeptidase from White-Rot Basidiomycetes *Phanerochaete chrysosporium*. *Biochimie* **2010**, *92*, 779–788. [CrossRef]
21. Alonso, J.; Garća, J.L. Proline Iminopeptidase Gene from *Xanthomonas campestris pv. citri*. *Microbiology* **1996**, *142*, 2951–2957. [CrossRef]
22. Basten, D.E.J.W.; Moers, A.P.H.A.; van Ooyen, A.J.J.; Schaap, P.J. Characterisation of *Aspergillus niger* Prolyl Aminopeptidase. *Mol. Genet. Genom.* **2005**, *272*, 673–679. [CrossRef] [PubMed]
23. Kitazono, A.; Kitano, A.; Tsuru, D.; Yoshimoto, T. Isolation and Characterization of the Prolyl Aminopeptidase Gene (pap) from *Aeromonas sobria*: Comparison with the *Bacillus coagulans* Enzyme. *J. Biochem.* **1994**, *116*, 818–825. [CrossRef]
24. Kumar, S.; Stecher, G.; Li, M.; Knyaz, C.; Tamura, K. MEGA X: Molecular Evolutionary Genetics Analysis across Computing Platforms. *Mol. Biol. Evol.* **2018**, *35*, 1547–1549. [CrossRef] [PubMed]
25. Feller, G. Psychrophilic Enzymes: From Folding to Function and Biotechnology. *Scientifica* **2013**, *2013*, 512840. [CrossRef] [PubMed]
26. Cavicchioli, R.; Charlton, T.; Ertan, H.; Omar, S.M.; Siddiqui, K.S.; Williams, T.J. Biotechnological Uses of Enzymes from Psychrophiles. *Microb. Biotechnol.* **2011**, *4*, 449–460. [CrossRef]
27. Ding, G.W.; Zhou, N.D.; Tian, Y.P. Over-Expression of a Proline Specific Aminopeptidase from *Aspergillus oryzae* JN-412 and Its Application in Collagen Degradation. *Appl. Biochem. Biotechnol.* **2014**, *173*, 1765–1777. [CrossRef] [PubMed]
28. Ito, K.; Inoue, T.; Kabashima, T.; Kanada, N.; Huang, H.S.; Ma, X.; Azmi, N.; Azab, E.; Yoshimoto, T. Substrate Recognition Mechanism of Prolyl Aminopeptidase from *Serratia marcescens*. *J. Biochem.* **2000**, *128*, 673–678. [CrossRef]
29. Medrano, F.J.; Alonso, J.; Garcia, J.L.; Bode, W.; Gomis-Ruth, F.X. Crystallization and Preliminary X-Ray Diffraction Analysis of Proline Iminopeptidase from *Xanthomonas campestris pv. citri*. *FEBS Lett.* **1997**, *400*, 91–93. [CrossRef]

30. Paredes, D.; Watters, K.; Pitman, J.D.; Bystroff, C.; Dordick, S.J. Comparative void-volume analysis of psychrophilic and mesophilic enzymes: Structural bioinformatics of psychrophilic enzymes reveals sources of core flexibility. *BMC Struct. Biol.* **2011**, *11*, 42. [CrossRef]
31. Gou, R.; Cang, Z.; Yao, J.; Kim, M.; Deans, E.; Wei, G.; Kang, S. Structural cavities are critical to balancing stability and activity of a membrane-integral enzyme. *Proc. Natl. Acad. Sci. USA* **2020**, *117*, 22146–22156.
32. Raymond-Bouchard, I.; Goordial, J.; Zolotarov, Y.; Ronholm, J.; Stromvik, M.; Bakermans, C.; Whyte, G.L. Conserved genomic and amino acid traits of cold adaptation in subzero-growing Arctic permafrost bacteria. *FEMS Microbiol. Ecol.* **2018**, *94*, fiy023. [CrossRef] [PubMed]
33. Bharudin, I.; Zaki, N.Z.; Abu Bakar, F.D.; Mahadi, N.M.; Najimudin, N.; Illias, R.M.; Murad, A.M.A. Comparison of RNA extraction methods for transcript analysis from the psychrophilic yeast, *Glaciozyma antarctica*. *Malays. Appl. Biol.* **2014**, *3*, 71–80.
34. Edgar, R.C. MUSCLE: A Multiple Sequence Alignment Method with Reduced Time and Space Complexity. *BMC Bioinform.* **2004**, *5*, 113. [CrossRef] [PubMed]
35. Waterhouse, A.M.; Procter, J.B.; Martin, D.M.A.; Clamp, M.; Barton, G.J. Jalview Version 2—A Multiple Sequence Alignment Editor and Analysis Workbench. *Bioinformatics* **2009**, *25*, 1189–1191. [CrossRef]
36. Jaafar, N.R.; Littler, D.; Beddoe, T.; Rossjohn, J.; Illias, R.M.; Mahadi, N.M.; Mackeen, M.M.; Murad, A.M.A.; Abu Bakar, F.D. Crystal Structure of Fuculose Aldolase from the Antarctic Psychrophilic Yeast *Glaciozyma antarctica* PI12. *Acta Crystallogr. Sect. F Struct. Biol. Commun.* **2016**, *72*, 831–839. [CrossRef]
37. Adams, P.D.; Afonine, P.V.; Bunkóczi, G.; Chen, V.B.; Echols, N.; Headd, J.J.; Hung, L.-W.; Jain, S.; Kapral, G.J.; Grosse Kunstleve, R.W.; et al. The Phenix Software for Automated Determination of Macromolecular Structures. *Methods* **2011**, *55*, 94–106. [CrossRef]